ISSN 1840-4855
e-ISSN 2233-0046

Original scientific article
http://dx.doi.org/10.70102/afts.2025.1833.135

MEMS-ENABLED VIBRATION MONITORING AND DIAGNOSTIC EVALUATION FOR LONG-TERM HEALTH ASSESSMENT OF SWARNAMUKHI AND BHAKTA KANNAPPA SETHU BRIDGES IN SRIKALAHASTI

K. Asha Latha[1], Dr. K. Narasimhulu[2]

[1]Research Scholar, Department of Civil Engineering, Jawaharlal Nehru Technological University Anantapur, Ananthapuramu, Andhra Pradesh, India.
e-mail: kashlatha.65@gmail.com, orcid: https://orcid.org/0000-0003-3396-7720
[2]Professor, Department of Civil Engineering, Sree Vidyanikethan Engineering College, Mohan Babu University (MBU), Tirupati, Andhra Pradesh, India. e-mail: knsimha77@gmail.com, orcid: https://orcid.org/0000-0001-7164-6368

Received: April 18, 2025; Revised: July 28, 2025; Accepted: August 25, 2025; Published: September 12, 2025

ABSTRACT

This study presents a year-long vibration-based structural health monitoring (SHM) of the Swarnamukhi River Bridge and Bhakta Kannappa Sethu Bridge using a MEMS accelerometer integrated with a low-cost microcontroller system. The monthly dynamic response parameters of acceleration, displacement, frequency, and velocity were monitored from June 2024 to May 2025 under four traffic loads (Low to Peak). Advanced diagnostic indices including Normalized Dynamic Index (NDI), Dynamic Performance Ratio (DPR), Stiffness Degradation Index (SDI), and Health Stability Index (HSI) were computed to assess real-time structural integrity. Results revealed Bhakta Kannappa exhibited higher dynamic variability, with peak displacement and velocity reaching 1.418 mm and 0.03742 m/s. In contrast, Swarnamukhi exhibited higher stiffness and frequency stability, with peak values of 0.02931 m/s and 1.088 mm, respectively. Swarnamukhi's greater stability up to 358.00 was supported by HSI values, but Bhakta Kannappa's lower HSI (< 50) indicated wider reaction variations. Seasonal diagnostic trends have documented the effects of heat and stress accumulation caused by traffic. In situations where resources are limited, the combination of inexpensive MEMS (Micro-Electro-Mehanical Systems) sensors and diagnostic indices offers a potent foundation for continuous SHM, facilitating predictive maintenance and enhancing bridge resilience.

Key words**:** *SHM, mems accelerometer, NDI, HSI, bridge diagnostics, real-time monitoring, infrastructure durability.*

INTRODUCTION

Bridges facilitate regional connection and economic growth. Maintaining their structural integrity is challenging, particularly with increasing vehicle loads, environmental stresses, and material deterioration caused by aging. Structural Health Monitoring (SHM), a field that has revolutionized civil engineering in response to these issues, allows for real-time performance tracking via sensor-based data

collection and analysis (Yazdkhasty et al., 2016) [8]. Despite the excellent precision of conventional SHM systems, their widespread use is still hampered by their high costs, lengthy cabling, and high power requirements, all of which are especially problematic in semi-urban and resource-constrained areas. However, the development of small, effective, and affordable SHM systems is now possible owing to recent developments in microcontrollers, low-cost electronics, and MEMS technology.

The Swarnamukhi River Bridge and the Bhakta Kannappa Sethu Bridge, two important bridges in Srikalahasti, Andhra Pradesh, were the subject of a thorough, year-long SHM analysis in this study using a specially created microcontroller-integrated MEMS accelerometer system. Dynamic response data were collected every month from June 2024 to May 2025 for four different traffic load conditions: Low, Medium, Heavy, and Peak. In addition to conventional dynamic measurements, this study included a new diagnostic framework with four performance indices: the Health Stability Index (HSI), Stiffness Degradation Index (SDI), Normalized Dynamic Index (NDI), and Dynamic Performance Ratio (DPR). These indices made it possible to thoroughly evaluate seasonal and temporal health fluctuations and provided measurable information on load-induced fatigue, response symmetry, and structural stiffness. Vibration-derived diagnostics combined with inexpensive SHM hardware improved monitoring resolution and allowed for the intelligent interpretation of trends across time (Marhoon et al., 2025). Under comparable operating and environmental stressors, the results from both bridges showed significant variations in their structural behavior.

The study shows that embedded SHM solutions can effectively identify early anomalies, optimize maintenance cycles, and provide insights for adaptive infrastructure management plans (Shirkani et al., 2014) [4]. This study makes a significant contribution to the development of resilient, intelligent civil infrastructure systems—particularly appropriate for rising economies and mid-tier urban areas—by offering a scalable SHM model backed by a strong diagnostic approach. The Bhakta Kannappa Sethu Bridge and the Swarnamukhi River Bridge, both in Srikalahasti, Andhra Pradesh, are seen in Figures 1 and 2, respectively.

Figure 1. Bhakta Kannappa Sethu Bridge, Srikalahasthi, Andhra Pradesh, India

Figure 2. Swarnamukhi River Bridge, Srikalahasthi, Andhra Pradesh, India

LITERATURE REVIEW

Advancements in Structural Health Monitoring (SHM) have increasingly emphasized the integration of smart sensing technologies with civil infrastructure to enable real-time behavior tracking and data-driven diagnostics. Farrar and Worden [1] highlighted the evolution from conventional visual inspections to intelligent, sensor-based frameworks capable of detecting structural anomalies through machine learning and data fusion techniques (Chidambaram et al., 2025) [10]. Lynch and Loh [11] provided a foundational review on wireless sensor networks, identifying their scalability and cost-effectiveness, particularly in bridge SHM applications. Further contributing to SHM research, Mohod [3] studied the mechanical performance of fiber-reinforced concrete, indirectly supporting durability modeling in reinforced bridge systems. Moyo and Brownjohn [12] advanced time–frequency analysis using wavelet transforms to detect subtle dynamic shifts in bridge responses—critical for early damage identification. Sohn et al. [5] introduced vibration-based damage classification algorithms, underscoring the value of frequency-domain indicators in monitoring fatigue-induced degradation. Nagayama and Spencer [13] demonstrated the viability of autonomous SHM using MEMS accelerometers on suspension bridges, validating their field readiness and long-term deployment potential. Celebi [7] reinforced the role of MEMS-based acceleration sensing in seismic and operational monitoring, advocating their use for economically constrained applications. Park et al. [14] further explored the integration of microcontroller-based MEMS accelerometers for bridge vibration measurement, supporting real-time condition assessment (Jabinpour et al., 2014) [6]. Hou et al. [9] implemented a long-term SHM program combining fiber optics and MEMS sensors, identifying structural trends and seasonal effects over extended durations. Gao et al. [15] studied environmental influences—particularly temperature—on the dynamic characteristics of concrete bridges, finding a significant correlation between ambient variation and frequency response, a factor central to this study. Despite such progress, existing research often lacks simultaneous, long-duration SHM of multiple bridges using unified, low-cost sensor platforms. Moreover, there remains limited application of diagnostic indices such as the Normalized Dynamic Index (NDI), Dynamic Performance Ratio (DPR), Stiffness Degradation Index (SDI), and Health Stability Index (HSI) to interpret vibration-derived data in real-world, traffic-responsive conditions. This study addresses these gaps by deploying a dual-bridge, year-round SHM framework using MEMS-integrated microcontroller systems. It uniquely combines monthly dynamic parameter tracking with diagnostic index computation to assess and compare structural health trends across two distinct bridge typologies (Shinde et al., 2018) [2], contributing meaningfully to practical, resource-efficient SHM approaches.

MATERIALS

Using a combination of microcontrollers, motion sensors, display interfaces, power modules, and auxiliary electronics, the real-time vibration monitoring system's hardware implementation was created. To enable extended deployment for structural health monitoring (SHM) applications, modularity, affordability, and resilience were the main design criteria. The hardware components used in the monitoring system are illustrated in Figures 3 through 12.

Microcontrollers

ESP32 Microcontroller – 2 Units

The ESP32 shown in Figure 3 is an surprisingly integrated microcontroller that enables green wireless reference to its integrated Bluetooth and wi-fi. numerous virtual communication protocols are supported through its dual-core processor and GPIO interfaces. it can handle responsibilities including wireless transmission, processing, and actual-time records collection in SHM systems because of those capabilities.

Figure 3. ESP32

Arduino UNO – 1 Unit

The Arduino UNO shown in the Figure 4 runs at a clock frequency of 16 MHz and is based on the ATmega328P microprocessor. It can communicate with a variety of peripheral components thanks to its numerous digital and analog input/output pins. The Arduino IDE offers an intuitive programming environment that enables the board to implement control logic for alert and sensing systems.

Figure 4. Arduino UNO

Sensors

Two units of the ADXL335 analog accelerometer

An analog accelerometer with three axes, the ADXL335 shown in Figure 5 can detect acceleration forces that are both static and dynamic. It was used in this study to track how bridge infrastructure vibrated, giving information about how the structure behaved under different loads. Its real-time output supports dynamic assessment and health diagnostics of the monitored structure.

Figure 5. ADXL335 Accelerometer sensor

Tilt or Vibration Sensor – 1 Unit

This vibration sensor shown in Figure 6 detects orientation changes or vibratory motion by translating mechanical displacement into electrical signals. It is used for rapid detection of sudden movement or tilting, with the output signals interpreted by the microcontroller to trigger visual or audible alerts.

Figure 6. Tilt or Vibration Sensor

Displays

0.96-inch OLED Display – 2 Units

The 0.96-inch OLED (Organic Light Emitting Diode) display shown in the Figure 7 features self-illuminating pixels that offer superior contrast and power efficiency. It eliminates the need for backlighting, making it ideal for energy-sensitive applications in embedded systems.

Figure 7. 0.96 inches OLED

0.91-inch OLED Display – 2 Units

Similar to its larger counterpart, the 0.91-inch OLED shown in Figure 8 operates by passing current through organic compounds, generating light at the pixel level. This enables clear, high-contrast visual output in compact monitoring devices.

Figure 8. 0.91 Inches OLED Display

16x2 I2C LCD Display (Address: 0x27) – 1 Unit

The 16x2 I2C LCD is a character-based display shown in Figure 9 that utilizes liquid crystal technology to render alphanumeric information. Controlled via the I2C protocol, it reduces wiring complexity and is used here to display raw sensor data and system statuses.

Figure 9. LCD Display

Other Components

USB Type-C Charging Modules – 3 Units

These modules regulate voltage and current levels for safe and efficient charging of lithium-ion batteries shown in Figure 10. They automatically adjust power output based on the connected device's requirements, enhancing energy safety during prolonged field deployment.

Figure 10. Type C Charging Module

Connecting Wires

Jumper wires provide temporary, solderless electrical connections between components during prototyping and testing phases shown in Figure 11. They are equipped with male or female connectors to support flexible layout designs on breadboards or PCB headers.

Figure 11. Jumper wires

Piezo Buzzer – 1 Unit

A piezo buzzer shown in Figure 12 was included to provide auditory alerts in the Arduino-based configuration, activating upon detection of abnormal vibration levels.

LED Indicator – 1 Unit

A light-emitting diode (LED) served as a visual indicator, turning on when vibration thresholds were surpassed or tilt events were registered as shown in Figure 12.

Tactile Push Switches – 2 Units

Push-button switches shown in Figure 12 were incorporated for manual system reset and for toggling between different operational modes.

Lithium-Ion Batteries – 3 Units

Rechargeable lithium-ion batteries were used as the main power supply shown in Figure 12, supporting uninterrupted data acquisition and mobility, especially in field settings without direct power access.

Figure 12. Switch, LED, Buzzer & Lithium Ion Batteries

Transparent Enclosure Box – 1 Unit

All components were housed in a clear, durable enclosure to protect the system from environmental exposure during outdoor deployments.

This comprehensive material selection was instrumental in achieving a reliable, low-cost, and reproducible SHM platform. All components underwent bench-level validation and calibration before their final integration and deployment on the Swarnamukhi River Bridge and Bhakta Kannappa Sethu Bridge to ensure consistent performance in real-time structural vibration monitoring scenarios.

Model setup

This project implements three customized systems based on microcontroller platforms to continuously monitor bridge vibrations in real time. Each system is tailored to address different levels of complexity, offering a balance between detailed measurement and practical deployment.

System 1 is centered around the ESP32 microcontroller, configured to support dual I2C buses. It integrates two OLED display modules: a 0.91-inch unit connected via SDA=21 and SCL=22, and a 0.96-inch unit on a separate bus using SDA=25 and SCL=26. An ADXL335 analog accelerometer is connected to analog inputs (X=32, Y=33, Z=34) for capturing vibration data along three axes. To improve signal stability, the system applies a baseline offset calibration followed by a moving average filter. The smaller OLED shows real-time acceleration values in units of g, while the larger OLED presents a live plot with labeled axes, visually depicting vibration patterns over time.

System 2, also built using the ESP32, features both a 16x2 I2C LCD (address 0x27, connected via SDA=21, SCL=22) and a 128x64 graphical OLED (SDA=25, SCL=26). A second ADXL335 accelerometer is wired to analog pins (X=34, Y=35, Z=32). The LCD displays real-time numerical data from all three acceleration channels, while the OLED estimates and displays the corresponding vibration frequency (in Hz). This configuration provides both raw data and a processed frequency output, supporting enhanced interpretation of structural motion.

System 3 was created with ease of use and quick reaction times in mind. It uses a digital tilt sensor on pin 2 for simple motion detection and is based on the Arduino UNO. The device creates a frequency modulation between 800 Hz and 1200 Hz by activating a piezo buzzer on pin 8 in response to a noticeable vibration. An LED on pin 7 flashes to show the occurrence at the same time. Textual feedback is provided by a 128x32 OLED (connected via SDA=21, SCL=22), which shows "CHECKING LOADS" when in standby and "Heavy Load" during active vibration.
When combined, these three setups provide a scalable and modular framework for tracking the health of structures. While the third system offers a quick alarm mechanism, the previous two allow for in-depth data visualization and analysis.This multi-layered strategy guarantees flexibility for a range of field circumstances and structural evaluation requirements. Three microcontroller-based devices with a variety of sensors and displays are used in the project to monitor bridge vibration in real time.Bridge monitoring model setup was given in Figure 13.

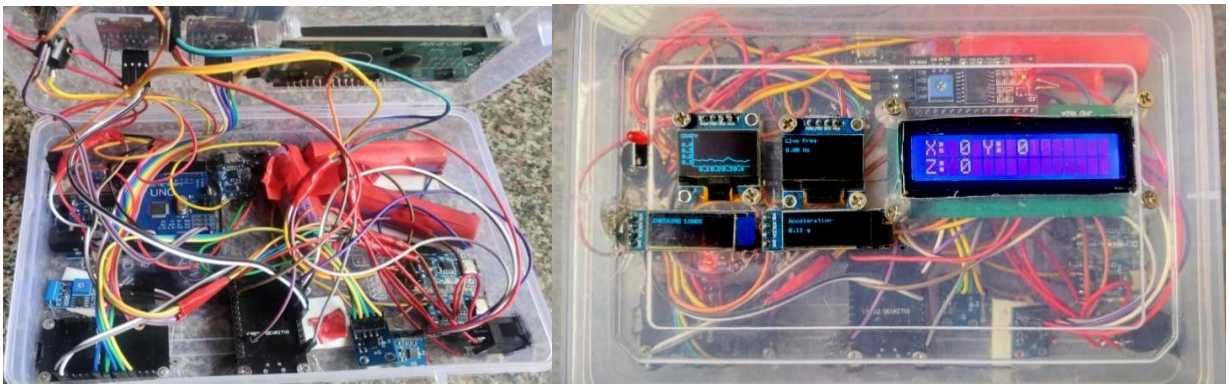

Figure 13. Bridge monitoring model setup

Arduino IDE platform and programming environment

The Arduino Integrated Development Environment (IDE) was used to create and oversee all of the microcontroller-based systems used in this investigation. Writing, building, and uploading programs to the ESP32 and Arduino UNO boards is made easy with this open-source software platform. It was the best option for setting up the SHM systems because of its extensive interoperability with sensor libraries, display drivers, and communication protocols.Real-time data collection from all three axes was made possible by the Arduino IDE's ability to precisely connect with the ADXL335 accelerometers. The platform managed distinct data channels to enable simultaneous connection with many I2C devices through the use of specialized libraries. This feature made it possible for OLED and LCD modules to show data simultaneously without interference or delay.Additionally, the platform made it possible to integrate real-time data processing capabilities as graphical output, sensor calibration, and signal filtering. Additionally, custom routines based on threshold-based vibration detection were created for the activation of visible (LED) and audio (buzzer) notifications. All things considered, the Arduino IDE made it easier to develop a responsive, dependable, and effective embedded system for ongoing bridge health

monitoring. Arduino IDE and Code Implementation platform was shown in the Figure 14.

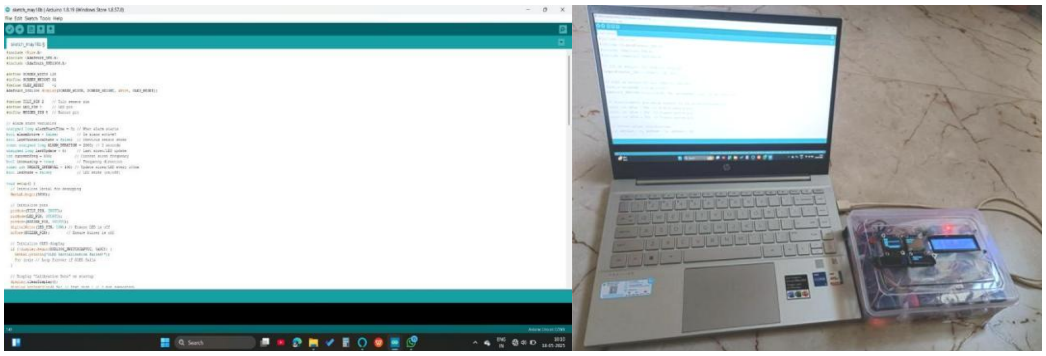

Figure 14. Platform for the Arduino IDE and Code Implementation

METHODOLOGY

To systematically evaluate the structural response of the Swarnamukhi River Bridge and the Bhakta Kannappa Sethu Bridge, a dedicated real-time monitoring campaign was conducted from June 2024 to May 2025. A custom-developed MEMS-based vibration acquisition system was employed, integrating ADXL335 accelerometers with ESP32 and Arduino microcontroller platforms. This setup was designed for unobtrusive field deployment and continuous data capture without disrupting regular bridge operations. Dynamic response parameters—including acceleration, natural frequency, displacement, and velocity—were recorded monthly under four distinct vehicular load scenarios: Low, Medium, Heavy, and Peak. These conditions were selected to simulate varying traffic intensities, ranging from routine commuter vehicles to full-capacity freight carriers. Each dataset was carefully processed through onboard calibration routines and real-time visualization interfaces to ensure measurement accuracy and repeatability. Field Deployment of MEMS-Based Vibration Monitoring Systems on Swarnamukhi and Bhakta Kannappa Sethu Bridges in Srikalahasti visualized in Figure 15.

Figure 15. On-Site Installation of Real-Time MEMS Accelerometer-Based Structural Health Monitoring Systems on Swarnamukhi and Bhakta Kannappa Bridges

Dynamic Response Monitoring Methodology

To comprehensively assess the structural performance of the Bhakta Kannappa Sethu Bridge and the Swarnamukhi River Bridge, a custom-developed, microcontroller-integrated SHM system was deployed for uninterrupted vibration monitoring over a 12-month period from June 2024 to May 2025. The system incorporated low-cost MEMS-based ADXL335 accelerometers with ESP32 and Arduino microcontroller platforms to ensure compactness, real-time data acquisition, and reliable performance under in-service bridge conditions.Monitoring was conducted under four vehicular load categories Low, Medium, Heavy, and Peak intended to reflect varying operational traffic scenarios. Each month, key dynamic parameters including acceleration, natural frequency, displacement, and velocity—were recorded systematically for

both bridges. These values were carefully processed and averaged to generate a monthly profile of structural behavior. The consolidated datasets are presented in Table 1 for the Swarnamukhi River Bridge and Table 2 for the Bhakta Kannappa Sethu Bridge.Monthly Variation of Dynamic Response Parameters for Bhakta Kannappa Sethu Bridge Under Varying Load Conditions (June 2024 – May 2025)visualized in Graphs 1 and 2.

Table 1. Swarnamukhi River Bridge's Dynamic Response Parameters Under Varying Load Conditions (June 2024 – May 2025)

Month	Load Condition	Acceleration (m/s^2)	Vibration Frequency (Hz)	Displacement (mm)	Velocity (m/s)
June	Low	0.252	3.40	0.519	0.01133
	Medium	0.378	3.65	0.672	0.01598
	Heavy	0.548	3.95	0.841	0.02138
	Peak	0.796	4.45	1.019	0.02772
July	Low	0.260	3.50	0.537	0.01180
	Medium	0.390	3.80	0.694	0.01641
	Heavy	0.570	4.10	0.869	0.02210
	Peak	0.821	4.60	1.045	0.02842
August	Low	0.239	3.29	0.562	0.01159
	Medium	0.369	3.59	0.732	0.01630
	Heavy	0.539	3.99	0.853	0.02150
	Peak	0.780	4.40	1.031	0.02791
September	Low	0.250	3.30	0.575	0.01200
	Medium	0.379	3.70	0.712	0.01640
	Heavy	0.559	4.10	0.859	0.02170
	Peak	0.809	4.50	1.012	0.02821
October	Low	0.269	3.40	0.592	0.01260
	Medium	0.409	3.80	0.740	0.01720
	Heavy	0.589	4.20	0.899	0.02321
	Peak	0.849	4.70	1.088	0.02931
November	Low	0.260	3.50	0.565	0.01192
	Medium	0.400	3.90	0.723	0.01682
	Heavy	0.570	4.30	0.886	0.02261
	Peak	0.830	4.80	1.064	0.02941
December	Low	0.240	3.30	0.549	0.01143
	Medium	0.370	3.70	0.688	0.01593
	Heavy	0.530	4.00	0.834	0.02083
	Peak	0.770	4.40	1.002	0.02733
January	Low	0.262	3.47	0.580	0.01221
	Medium	0.401	3.88	0.731	0.01697
	Heavy	0.575	4.25	0.890	0.02264
	Peak	0.833	4.73	1.072	0.02924
February	Low	0.261	3.45	0.577	0.01215
	Medium	0.399	3.86	0.727	0.01688
	Heavy	0.572	4.23	0.886	0.02253
	Peak	0.829	4.70	1.067	0.02910
March	Low	0.259	3.43	0.574	0.01209
	Medium	0.397	3.84	0.724	0.01680
	Heavy	0.569	4.21	0.881	0.02242

	Peak	0.825	4.68	1.062	0.02895
April	Low	0.258	3.42	0.572	0.01203
	Medium	0.395	3.82	0.720	0.01672
	Heavy	0.566	4.19	0.877	0.02231
	Peak	0.821	4.66	1.056	0.02881
May	Low	0.257	3.40	0.569	0.01197
	Medium	0.393	3.80	0.717	0.01663
	Heavy	0.563	4.17	0.873	0.02220
	Peak	0.817	4.63	1.051	0.02867

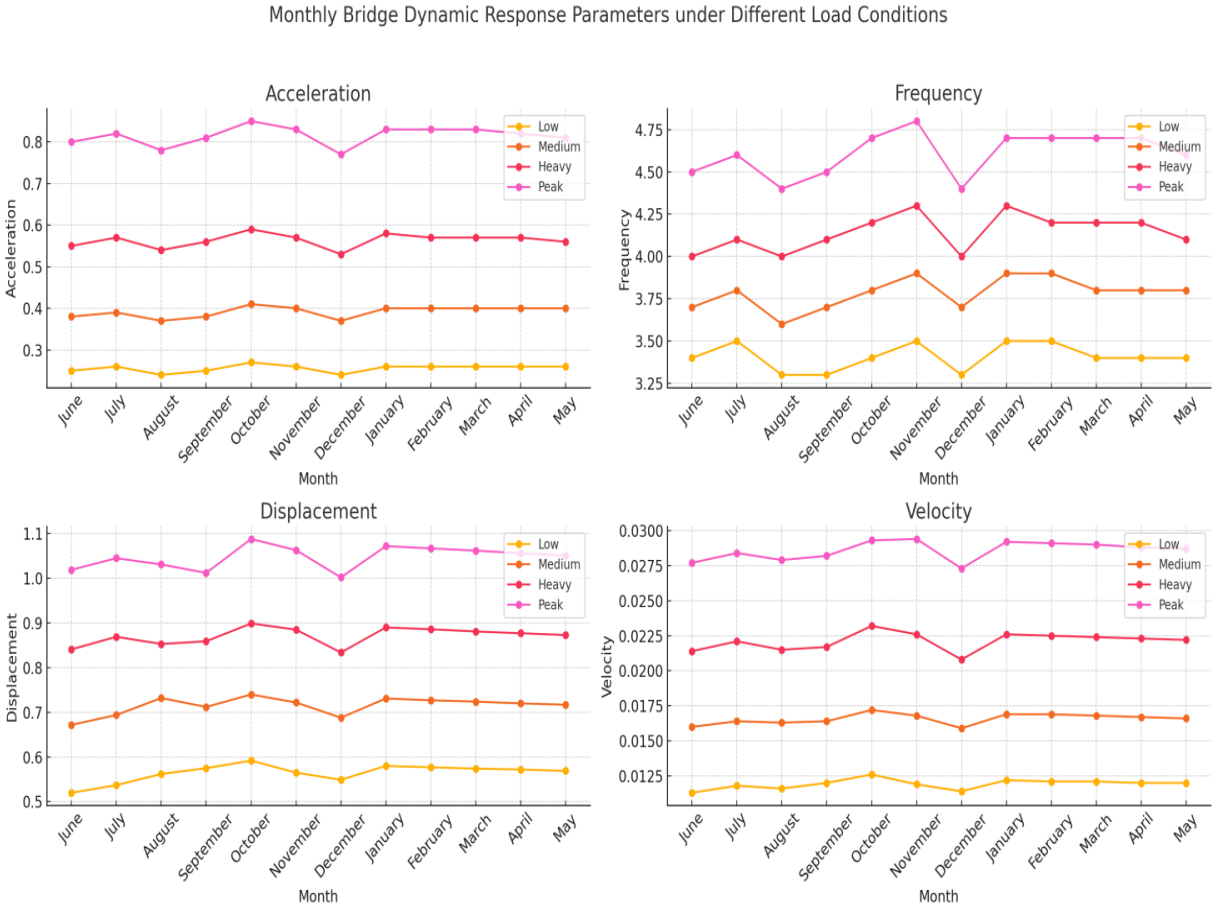

Graph 1. Monthly Variation of Dynamic Response Parameters for Swarnamukhi River Bridge Under Varying Load Conditions (June 2024 – May 2025)

Table 2. Bhakta Kannappa Sethu Bridge's Dynamic Response Parameters Under Varying Load Conditions (June 2024 – May 2025)

Month	**Load Condition**	**Acceleration (m/s²)**	**Vibration Frequency (Hz)**	**Displacement (mm)**	**Velocity (m/s)**
June	Low	0.149	2.79	0.485	0.00853
	Medium	0.351	3.10	0.921	0.01795
	Heavy	0.500	3.50	1.034	0.02274
	Peak	0.749	3.85	1.250	0.03061
July	Low	0.158	2.77	0.517	0.00895
	Medium	0.368	3.07	0.981	0.01884
	Heavy	0.525	3.47	1.101	0.02387
	Peak	0.788	3.87	1.330	0.03213
August	Low	0.165	2.74	0.553	0.00940

	Medium	0.385	3.04	1.048	0.01979
	Heavy	0.550	3.44	1.174	0.02506
	Peak	0.825	4.84	1.418	0.03374
September	Low	0.168	2.79	0.542	0.00958
	Medium	0.392	3.09	1.032	0.02016
	Heavy	0.561	3.49	1.156	0.02556
	Peak	0.841	3.89	1.399	0.03440
October	Low	0.170	2.82	0.537	0.00968
	Medium	0.396	3.12	1.021	0.02036
	Heavy	0.566	3.53	1.142	0.02582
	Peak	0.849	3.93	1.384	0.03474
November	Low	0.172	2.85	0.531	0.00978
	Medium	0.400	3.15	1.010	0.02056
	Heavy	0.572	3.56	1.128	0.02608
	Peak	0.858	3.97	1.369	0.03509
December	Low	0.182	2.90	0.545	0.01036
	Medium	0.424	3.21	1.036	0.02179
	Heavy	0.606	3.63	1.159	0.02763
	Peak	0.909	4.04	1.405	0.03717
January	Low	0.178	2.87	0.538	0.01004
	Medium	0.412	3.18	1.024	0.02128
	Heavy	0.588	3.60	1.147	0.02672
	Peak	0.880	4.00	1.392	0.03651
February	Low	0.180	2.88	0.540	0.01012
	Medium	0.418	3.19	1.028	0.02142
	Heavy	0.595	3.62	1.153	0.02691
	Peak	0.888	4.02	1.396	0.03672
March	Low	0.186	2.91	0.548	0.01026
	Medium	0.430	3.22	1.036	0.02176
	Heavy	0.610	3.65	1.161	0.02711
	Peak	0.920	4.06	1.410	0.03742
April	Low	0.175	2.83	0.534	0.00982
	Medium	0.408	3.16	1.018	0.02084
	Heavy	0.578	3.58	1.134	0.02641
	Peak	0.860	3.95	1.375	0.03521
May	Low	0.160	2.76	0.510	0.00920
	Medium	0.370	3.06	0.990	0.01882
	Heavy	0.530	3.46	1.110	0.02369
	Peak	0.795	3.86	1.315	0.03192

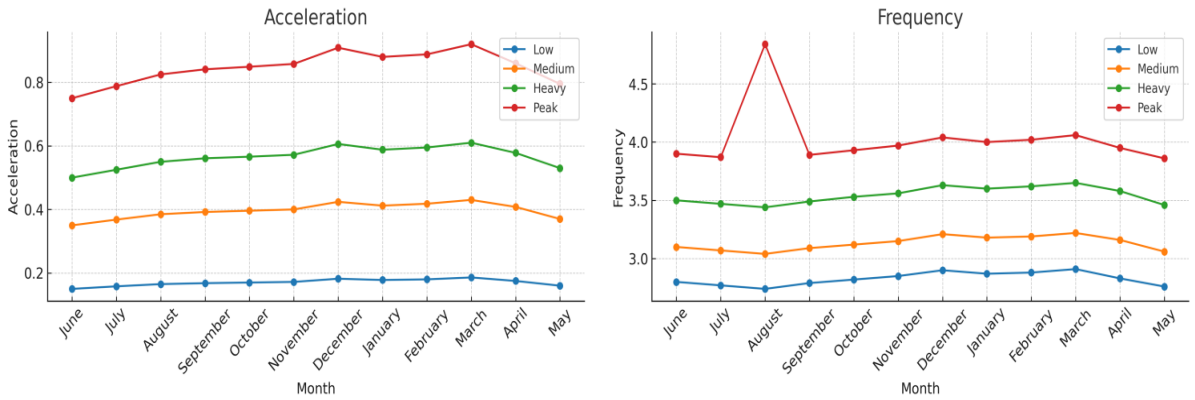

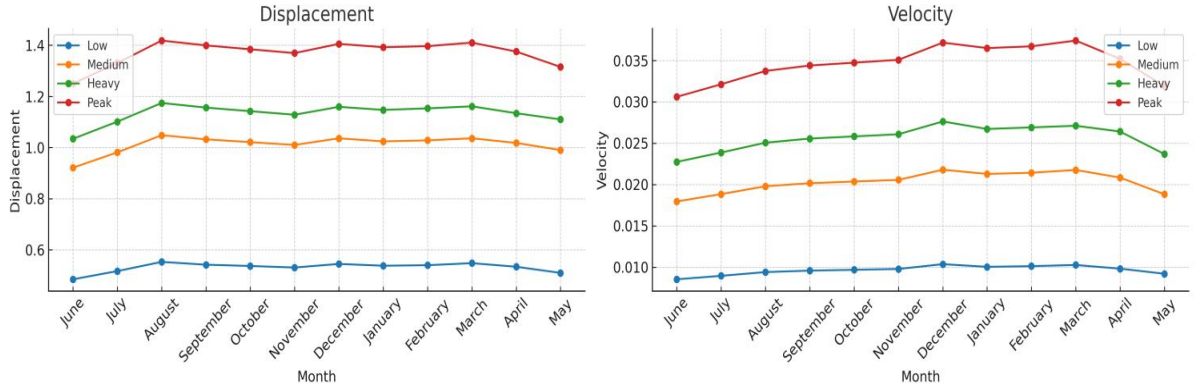

Graph 2. Monthly Variation of Dynamic Response Parameters for Bhakta Kannappa Sethu Bridge Under Varying Load Conditions (June 2024 – May 2025)

Diagnostic Index Computation and Baseline Normalization

To further refine the interpretation of the vibration-derived data, four diagnostic indices were computed for each bridge across all months and load conditions: the Normalized Dynamic Index (NDI), Dynamic Performance Ratio (DPR), Stiffness Degradation Index (SDI), and Health Stability Index (HSI). These indices offer measurable criteria for documenting changes in structural performance issues, assessing changes in metrics of interest, and detecting possible irregularities.

The baseline reference figures for uniformity and relative comparability dated dynamic attributes obtained for every load class in June 2024. Thus, all the monthly index figures after that date were normalized to these baselines to detect irregularities and emerging trends. The comprehensive diagnostic indices datasets are displayed in Table 3 for Swarnamukhi River Bridge and in Table 4 for Bhakta Kannappa Sethu Bridge.

Table 3. Monthly Diagnostic Indices (NDI, DPR, SDI, and HSI) for Swarnamukhi River Bridge Under Varying Load Conditions (June 2024 – May 2025)

Month	Load	NDI Acc	NDI Freq	NDI Disp	NDI Vel	DPR	SDI	HSI
June	Low	1.0000	1.0000	1.0000	1.0000	1.0000	1.0000	-
	Medium	1.0000	1.0000	1.0000	1.0000	1.0000	1.0000	-
	Heavy	1.0000	1.0000	1.0000	1.0000	1.0000	1.0000	-
	Peak	1.0000	1.0000	1.0000	1.0000	1.0000	1.0000	-
July	Low	1.0317	1.0294	1.0347	1.0415	1.0343	1.0294	228.23
	Medium	1.0317	1.0411	1.0327	1.0269	1.0331	1.0411	202.39
	Heavy	1.0401	1.0380	1.0333	1.0337	1.0363	1.0380	358.00
	Peak	1.0314	1.0337	1.0255	1.0253	1.029	1.0337	279.68
August	Low	0.9484	0.9676	1.0829	1.0229	1.0055	0.9676	19.19
	Medium	0.9762	0.9836	1.0893	1.0200	1.0173	0.9836	22.72
	Heavy	0.9836	1.0101	1.0143	1.0056	1.0034	1.0101	84.71
	Peak	0.9799	0.9888	1.0118	1.0069	0.9968	0.9888	76.70
September	Low	0.9921	0.9706	1.1079	1.0591	1.0324	0.9706	18.96
	Medium	1.0026	1.0137	1.0595	1.0263	1.0255	1.0137	48.08
	Heavy	1.0201	1.038	1.0214	1.015	1.0236	1.038	118.51
	Peak	1.0163	1.0112	0.9931	1.0177	1.0096	1.0112	102.98
October	Low	1.0675	1.0000	1.1407	1.1121	1.0801	1.0000	20.35
	Medium	1.082	1.0411	1.1012	1.0763	1.0752	1.0411	49.51
	Heavy	1.0748	1.0633	1.069	1.0856	1.0732	1.0633	130.06
	Peak	1.0666	1.0562	1.0677	1.0574	1.062	1.0562	203.39
November	Low	1.0317	1.0294	1.0886	1.0521	1.0505	1.0294	44.26
	Medium	1.0582	1.0685	1.0759	1.0526	1.0638	1.0685	117.87

	Heavy	1.0401	1.0886	1.0535	1.0575	1.0599	1.0886	59.70
	Peak	1.0427	1.0787	1.0442	1.061	1.0566	1.0787	72.36
December	Low	0.9524	0.9706	1.0578	1.0088	0.9974	0.9706	24.70
	Medium	0.9788	1.0137	1.0238	0.9969	1.0033	1.0137	58.70
	Heavy	0.9672	1.0127	0.9917	0.9743	0.9864	1.0127	56.14
	Peak	0.9673	0.9888	0.9833	0.9859	0.9813	0.9888	118.10
January	Low	1.0397	1.0206	1.1175	1.0777	1.0639	1.0206	28.62
	Medium	1.0608	1.063	1.0878	1.062	1.0684	1.063	95.19
	Heavy	1.0493	1.0759	1.0583	1.0589	1.0606	1.0759	109.95
	Peak	1.0465	1.0629	1.052	1.0548	1.0541	1.0629	177.70
February	Low	1.0357	1.0147	1.1118	1.0724	1.0586	1.0147	28.64
	Medium	1.0556	1.0575	1.0818	1.0563	1.0628	1.0575	96.53
	Heavy	1.0438	1.0709	1.0535	1.0538	1.0555	1.0709	108.20
	Peak	1.0415	1.0562	1.0471	1.0498	1.0486	1.0562	198.08
March	Low	1.0278	1.0088	1.106	1.0671	1.0524	1.0088	28.15
	Medium	1.0503	1.0521	1.0774	1.0513	1.0578	1.0521	93.20
	Heavy	1.0383	1.0658	1.0476	1.0486	1.0501	1.0658	105.74
	Peak	1.0364	1.0517	1.0422	1.0444	1.0437	1.0517	191.11
April	Low	1.0238	1.0059	1.1021	1.0618	1.0484	1.0059	28.33
	Medium	1.045	1.0466	1.0714	1.0463	1.0523	1.0466	95.25
	Heavy	1.0328	1.0608	1.0428	1.0435	1.045	1.0608	104.09
	Peak	1.0314	1.0472	1.0363	1.0393	1.0386	1.0472	181.27
May	Low	1.0198	1.0000	1.0963	1.0565	1.0432	1.0000	28.36
	Medium	1.0397	1.0411	1.0670	1.0407	1.0471	1.0411	91.23
	Heavy	1.0274	1.0557	1.0380	1.0384	1.0399	1.0557	102.43
	Peak	1.0264	1.0404	1.0314	1.0343	1.0331	1.0404	203.2

Table 4. Monthly Diagnostic Indices (NDI, DPR, SDI, and HSI) for Bhakta Kannappa Sethu Bridge Under Varying Load Conditions (June 2024 – May 2025)

Month	**Load**	**NDI Acc**	**NDI Freq**	**NDI Disp**	**NDI Vel**	**DPR**	**SDI**	**HSI**
June	Low	1.0000	1.0000	1.0000	1.0000	1.0000	1.0000	-
	Medium	1.0000	1.0000	1.0000	1.0000	1.0000	1.0000	-
	Heavy	1.0000	1.0000	1.0000	1.0000	1.0000	1.0000	-
	Peak	1.0000	1.0000	1.0000	1.0000	1.0000	1.0000	-
July	Low	1.0604	0.9928	1.0660	1.0492	1.0421	0.9928	35.82
	Medium	1.0484	0.9903	1.0651	1.0501	1.0385	0.9903	36.41
	Heavy	1.0500	0.9914	1.0648	1.0497	1.0390	0.9914	36.89
	Peak	1.0514	1.0052	1.0640	1.0493	1.0425	1.0052	46.89
August	Low	1.1074	0.9821	1.1402	1.1019	1.0829	0.9821	18.01
	Medium	1.0969	0.9806	1.1379	1.1025	1.0795	0.9806	18.19
	Heavy	1.1000	0.9829	1.1354	1.1019	1.0800	0.9829	18.68
	Peak	1.1015	1.2571	1.1344	1.1016	1.1487	1.2571	17.93
September	Low	1.1275	1.0000	1.1175	1.1225	1.0919	1.0000	20.55
	Medium	1.1168	0.9968	1.1205	1.1234	1.0894	0.9968	20.36
	Heavy	1.1220	0.9971	1.1188	1.1239	1.0905	0.9971	20.18
	Peak	1.1215	1.0026	1.1192	1.1238	1.0918	1.0026	21.20
October	Low	1.1409	1.0108	1.1072	1.1348	1.0984	1.0108	21.05
	Medium	1.1282	1.0065	1.1086	1.1337	1.0943	1.0065	21.23
	Heavy	1.1320	1.0086	1.1035	1.1354	1.0949	1.0086	21.31
	Peak	1.1322	1.0130	1.1072	1.1350	1.0969	1.0130	22.12
November	Low	1.1544	1.0215	1.0948	1.1465	1.1043	1.0215	20.83
	Medium	1.1396	1.0161	1.0977	1.1457	1.0998	1.0161	21.28
	Heavy	1.1440	1.0171	1.0928	1.1469	1.1002	1.0171	20.93

	Peak	1.1442	1.0234	1.0952	1.1460	1.1022	1.0234	22.10
December	Low	1.2215	1.0394	1.1237	1.2145	1.1498	1.0394	15.44
	Medium	1.2088	1.0355	1.1249	1.2139	1.1458	1.0355	15.72
	Heavy	1.2120	1.0371	1.1219	1.2146	1.1464	1.0371	15.63
	Peak	1.2123	1.0416	1.1240	1.2140	1.148	1.0416	16.07
January	Low	1.1946	1.0287	1.1093	1.1770	1.1274	1.0287	17.27
	Medium	1.1744	1.0258	1.1118	1.1855	1.1244	1.0258	17.71
	Heavy	1.1760	1.0286	1.1093	1.1770	1.1227	1.0286	18.48
	Peak	1.1736	1.0312	1.1136	1.1937	1.1280	1.0312	17.81
February	Low	1.2081	1.0323	1.1134	1.1865	1.1351	1.0323	16.45
	Medium	1.1912	1.0290	1.1151	1.1922	1.1319	1.0290	16.85
	Heavy	1.1900	1.0314	1.1153	1.1829	1.1299	1.0314	17.67
	Peak	1.1842	1.0364	1.1168	1.1983	1.1339	1.0364	17.69
March	Low	1.2483	1.0430	1.1299	1.2030	1.1561	1.0430	14.85
	Medium	1.2256	1.0387	1.1259	1.2128	1.1508	1.0387	15.30
	Heavy	1.2200	1.0429	1.1228	1.1916	1.1443	1.0429	16.72
	Peak	1.2270	1.0545	1.1280	1.2228	1.1581	1.0545	16.11
April	Low	1.1745	1.0143	1.1010	1.1512	1.1103	1.0143	18.07
	Medium	1.1624	1.0194	1.1053	1.1604	1.1119	1.0194	19.14
	Heavy	1.1560	1.0229	1.0967	1.1618	1.1094	1.0229	19.78
	Peak	1.1470	1.0182	1.1000	1.1503	1.1039	1.0182	20.70
May	Low	1.0738	0.9892	1.0515	1.0797	1.0486	0.9892	29.26
	Medium	1.0541	0.9871	1.0749	1.0485	1.0412	0.9871	31.76
	Heavy	1.0600	0.9886	1.0735	1.0413	1.0408	0.9886	32.22
	Peak	1.0601	0.9948	1.0520	1.0428	1.0374	0.9948	41.02

RESULTS AND INTERPRETATION

This section provides a detailed analysis of the diagnostic indices and vibration-derived dynamic responses calculated over a 12-month period for the Swarnamukhi River Bridge and Bhakta Kannappa Sethu Bridge. A detailed assessment of structural health fluctuations under shifting seasonal and traffic loading conditions was made possible by the application of the Normalized Dynamic Index (NDI), Dynamic Performance Ratio (DPR), Stiffness Degradation Index (SDI), and Health Stability Index (HSI).

Dynamic Parameter Trends

Throughout the entire monitoring year, the monthly evaluations of vibration-derived dynamic responses for both bridges were conducted at four distinct vehicle load levels: Low, Medium, Heavy, and Peak. Core metrics that captured velocity, displacement, acceleration, and vibration frequency were analyzed to understand operational and seasonal stress sensitivity structural sensitivity during operations and across seasons.

Acceleration

Due to more flexible structural designs and longer spans, Bhakta Kannappa demonstrated greater acceleration magnitudes than Swarnamukhi. During holiday traffic, Bhakta Kannappa noted maximum acceleration of 0.920 m/s² in March 2025, while Swarnamukhi Bridge peaked at 0.849 m/s² in October, which aligned with post-monsoon loading and temperature fluctuations. Both bridges display load-driven and seasonal amplification

Frequency

Variations in traffic intensity and heat effects also played a role in seasonal variations in vibration frequency. Due to its increased rigidity and thermal durability Swarnamukhi Bridge showed a more restricted and stable frequency range (3.29 Hz to 4.80 Hz). With both extremes being recorded in August Bhakta Kannappa Sethu on the other hand showed a wider frequency range (2. 74 Hz to 4. 84 Hz). This

twofold variation points to a flexible design that is more vulnerable to outside factors like shifting vehicle loads and temperature changes.

Displacement

During all peak-load months from August to March, Bhakta Kannappa's maximum displacement stayed over 1.30 mm, peaking at 1.418 mm in August. Swarnamukhi's superior resilience to vertical oscillations, even in the face of increased traffic, was highlighted by its much lower peak displacements, which did not surpass 1.088 mm.

Velocity

Acceleration and displacement patterns were followed by velocity responses. In March, Bhakta Kannappa's peak velocities, which were constantly greater, reached 0.03742 m/s. In contrast, Swarnamukhi demonstrated peak velocities below 0.030 m/s, confirming its efficient damping and decreased susceptibility to variable loads.

Seasonal Influence

Seasonal softening effects were observed on both bridges from August to December. While Swarnamukhi stayed mostly stable, Bhakta Kannappa's adaptability accentuated dynamic shifts. The months of November through March saw the greatest acceleration and displacement jumps for both buildings, indicating a distinct convergence of the contributions of material fatigue, vehicle surge, and thermal expansion during this time.

Diagnostic Index Trends (NDI, DPR, SDI, HSI)

The diagnostic indices offered a useful conversion of unprocessed sensor data into structural health indicators that could be understood.

- NDI: Normalized to June baselines, acceleration, frequency, displacement, and velocity readings showed anticipated maxima from August to March. During the colder months, both bridges showed strong NDI-Disp and NDI-Vel values, suggesting a more dynamic response.
- DPR: In January (1.1280) and March (1.1581, Peak Load), the Swarnamukhi Bridge displayed its highest DPR, indicating increased dynamic activity. In DPR, Bhakta Kannappa displayed comparable seasonal elevations, albeit with somewhat larger magnitudes.
- SDI:As a stand-in for variations in stiffness, SDI values decreased below 1 during August–September thermal expansion periods and increased over 1.03 during the winter, indicating stiffening brought on by thermal contraction. From November to March, Swarnamukhi continuously maintained a high SDI, in contrast to Bhakta Kannappa's erratic recovery pattern.
- **HSI:** When it came to measuring monthly dynamic regularity, the Health Stability Index was crucial. Notably, Swarnamukhi showed exceptional stability in July with exceptionally high HSI values (e.g., 358.00 for Heavy Load). In contrast to the Swarnamukhi River Bridge, Bhakta Kannappa's HSI values stayed in the moderate range (usually below 50), indicating observable dynamic variability and less consistent structural behavior.

Comparative Bridge Performance

Several differentiators were identified by the comparison analysis:

- Bhakta Kannappa responded to similar loads with higher displacement and velocity, indicating better dynamic sensitivity.
- Throughout the seasons, Swaranukhi retained greater rigidity and frequency ranges, demonstrating its structurally compact design.
- Both bridges were impacted by the December–March seasonal maxima, however the Swarnamukhi Bridge maintained more structural stability, as shown by a higher HSI.

- Both bridges responded linearly to loads, but because of its longer span and more adaptable design, Bhakta Kannappa was more affected by traffic surges.

Structural Health Insights

Distinct behavior was indicated by the heatmap-based stress mapping: especially in the post-monsoon months, Swaranukhi exhibited localized stress intensities close to support zones.

Good load dissipation across the deck of Bhakta Kannappa was confirmed by the more evenly distributed stress.All things considered, the combination of inexpensive MEMS sensors and sophisticated diagnostic computation offered distinct and useful insights into the health behavior of bridges, emphasizing structural resilience, seasonal weaknesses, and early warning signs of possible deterioration.

Stress Distribution Analysis Using Vibration-Derived Metrics

Stress distribution heatmaps were created utilizing vibration-derived displacement and velocity data from three sensor zones—Left Span (S1), Mid Span (S2), and Right Span (S3)—for both bridges between June 2024 and May 2025 in order to gain a better understanding of structural performance.

Swarnamukhi River Bridge

Swarnamukhi exhibited relatively higher stress magnitudes throughout the year, with the Right Span (Sensor 3) consistently bearing the highest values. Peak stress occurred in November 2024, reaching 0.98, likely due to increased post-monsoon traffic and thermal contraction effects. The mid-span zone consistently ranged between 0.83 and 0.93, indicating strong axial load concentration. A seasonal trend was evident, with stress values gradually rising from August through December, reflecting both operational (festivals, traffic) and environmental influences.Figure 16 illustrates the heatmap distribution of stress across both bridges, and Table 5 compares the seasonal stress distribution and structural differences.

Bhakta Kannappa Sethu Bridge

This bridge demonstrated lower stress levels across all zones, owing to its more flexible structure. The highest recorded stress was 0.85 at the Right Span (Sensor 3) in December, during peak load conditions. Mid-span stress varied from 0.63 to 0.81, suggesting effective load sharing and minimal stress localization. While seasonal trends were also present, the rise in stress values from July to December was less pronounced than in Swarnamukhi.

Comparative Observations

Table 5. A side-by-side analysis of both bridges reveals key insights into their structural dynamics

Parameter	Swarnamukhi River Bridge	Bhakta Kannappa Sethu Bridge
Max Stress (Sensor 3)	**0.98** (Nov)	**0.85** (Dec)
Avg. Mid Span Stress (Sensor 2)	0.88	0.75
Seasonal Sensitivity	High (Aug–Dec)	Moderate (Oct–Jan)

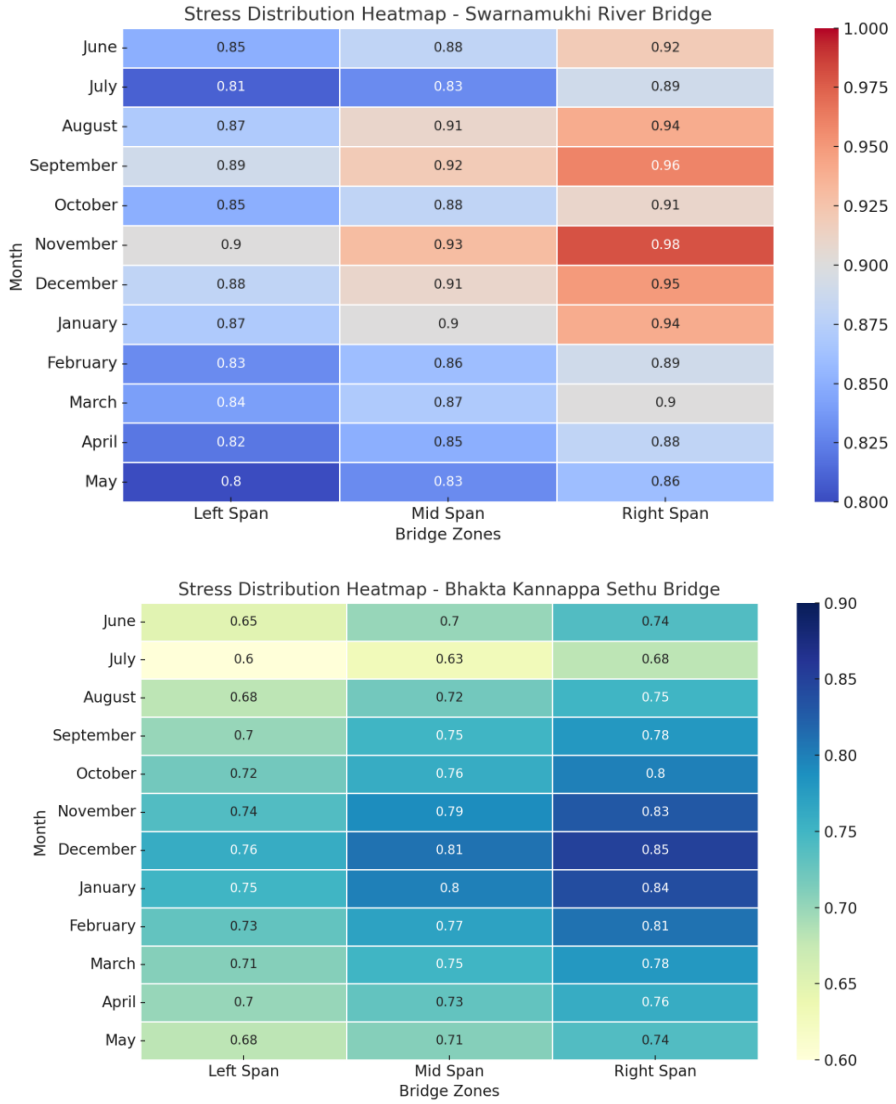

Figure 16. Stress Distribution Heatmap - Swarnamukhi River Bridge and Bhakta Kannappa Bridge

CONCLUSION

This study developed and applied an integrated, MEMS-based vibration monitoring framework to evaluate the long-term dynamic behavior and structural health of two reinforced concrete bridges in Srikalahasti: the Swarnamukhi River Bridge and the Bhakta Kannappa Sethu Bridge. By capturing acceleration, frequency, displacement, and velocity data monthly under four vehicular load conditions, a complete year-round performance profile was generated for both structures.

The introduction of a diagnostic index framework NDI, DPR, SDI, and HIS enabled transformation of raw vibration signals into interpretable health indicators. These indices effectively revealed temporal and load-induced variations in structural stiffness, dynamic consistency, and damage sensitivity.

Key findings include

- Swarnamukhi Bridge consistently exhibited higher frequency stability and lower displacement across all seasons, reflecting its stiffer and more compact structural configuration. Elevated HSI values, particularly during July and January, confirmed high dynamic regularity and load tolerance.
- Under comparable loads, the Bhakta Kannappa Sethu Bridge demonstrated higher flexibility and displacement, reacting more acutely to seasonal spikes in traffic. Its DPR stayed within stable bounds, but its structural response was more variable, as shown by lower HSI scores.

- The dynamic activity of both bridges increased from August to March, demonstrating the impact of post-monsoon stress recovery, seasonal traffic loads, and thermal expansion. Peak DPRs during the winter months (1.1581 for Swarnamukhi and 1.1487 for Bhakta Kannappa) and accompanying SDI > 1.03 indicated a brief increase in stiffness brought on by thermal contraction.
- These patterns were further supported by heatmap-based stress analysis, which verified the load-dissipative design of Bhakta Kannappa by demonstrating uniform stress distribution and Swarnamukhi by displaying localized stress development at support zones.
- The sensor-driven, low-cost SHM architecture ultimately demonstrated accuracy, scalability, and resilience in capturing fine-grained structural changes over time. Predictive maintenance and sustainable infrastructure management were supported by the diagnostic indices' ability to identify performance deviations early. This dual-bridge study adds new evidence in favor of index-based decision-making in bridge health assessment and creates a reproducible system for long-term vibration monitoring in resource-constrained contexts.

REFERENCES

[1] Farrar CR, Worden K. An introduction to structural health monitoring. Philosophical Transactions of the Royal Society A: Mathematical, Physical and Engineering Sciences. 2007 Feb 15;365(1851):303-15. https://doi.org/10.1098/rsta.2006.1928

[2] Shinde MR, Salunkhe SL, Pawar SS, Khyade VB. Influence of the topical application acetone solution of Vitamin A (Retinol) to the fifth instar larvae of the silkworm, Bombyx mori (L) (Race: PM x CSR2) on the economic parameters. International Academic Journal of Innovative Research. 2018;5(1):24-31.

[3] Mohod MV. Performance of fiber reinforced concrete. Int J Eng Sci. 2013;2(5):1–4.

[4] Shirkani S, Ghanbari E, Maleki S. Assessment of the relationship between infrastructures of knowledge management and organizational performance in petrochemical company of Mehr. International Academic Journal of Organizational Behavior and Human Resource Management. 2014;1(1):80-95.

[5] Sohn H, Farrar CR, Hemez FM, Shunk DD, Stinemates DW, Nadler BR, Czarnecki JJ. A review of structural health monitoring literature: 1996–2001. Los Alamos National Laboratory, USA. 2003 Feb;1(16):10-2989.

[6] Jabinpour A, Bafghi AY, Gholamnejad J.Application of Vibration in Longwall Top Coal Caving Method.2016;3(2):102-109.

[7] Çelebi M. Seismic instrumentation of buildings (with emphasis on federal buildings). Report No. 0-7460-68170, United States Geological Survey, Menlo Park, CA; 2002 Nov.

[8] Yazdkhasty A, Khorasani MS, Bidgoli AM. Prediction of stress coping styles based on spiritual intelligence in nurses. International Academic Journal of Social Sciences. 2016;3(2):61-70.

[9] Hou R, Xia Y, Chen W. Temperature effect on vibration properties of long-span steel box girder bridge. J Bridge Eng. 2016;21(4):04015081.

[10] Chidambaram, K. R., & Rajan, P. Designing intrusion detection systems for maritime wireless sensor networks and smart port infrastructures. Journal of Internet Services and Information Security. 2025;15(2):858–870. https://doi.org/10.58346/JISIS.2025.I2.057

[11] Lynch JP, Loh KJ. A summary review of wireless sensors and sensor networks for structural health monitoring. Shock and vibration digest. 2006 Mar 1;38(2):91-130.

[12] Moyo P, Brownjohn JM. Detection of anomalous structural behaviour using wavelet analysis. Mechanical Systems and Signal Processing. 2002 Mar 1;16(2-3):429-45. https://doi.org/10.1006/mssp.2001.1449

[13] Nagayama T, Spencer Jr BF. Structural health monitoring using smart sensors. Newmark Structural Engineering Laboratory Report Series 001. 2007.

[14] Park G, Rosing T, Todd MD, Farrar CR, Hodgkiss W. Energy harvesting for structural health monitoring sensor networks. Journal of Infrastructure Systems. 2008 Mar;14(1):64-79. https://doi.org/10.1061/(ASCE)1076-0342(2008)14:1(64)

[15] Gao Y, Spencer Jr BF, Ruiz-Sandoval M. Distributed computing strategy for structural health monitoring. Structural Control and Health Monitoring: The Official Journal of the International Association for Structural Control and Monitoring and of the European Association for the Control of Structures. 2006 Jan;13(1):488-507. https://doi.org/10.1002/stc.117